

Deriving Meaningful Equivalent Circuits for Electrically Small Multi-Conductor Structures

Lap K. Yeung*

Abstract—A new circuit reduction algorithm for generating physically meaningful equivalent circuits for electrically small structures is proposed in this work. It makes use of the generalized Y-to- Δ transformation as well as features unique to partial element equivalent circuits (PEECs) to perform the reduction process. For a given partial element equivalent circuit, insignificant nodes are removed one by one in a prioritized order according to both user-specified cut-off frequency and threshold value. By having the freedom of choosing these parameters, this algorithm provides users an option to make a tradeoff between accuracy and simplicity of the final reduced circuit. Since the generalized Y-to- Δ transformation can keep all mutual couplings intact, the order-reduced circuit should correctly capture all physical essences of the structure being modeled. Two examples are presented in this paper to validate the proposed algorithm. The equivalent circuits obtained can indeed reflect all essential physical features, demonstrating that the algorithm is a useful tool for designing and analyzing electrically small multi-conductor structures.

1. INTRODUCTION

The conventional partial element equivalent circuit (PEEC) [1] of a multi-conductor structure, even for a relatively simple one, is mesh-dependent and usually consists of a large number of elements. Such a circuit, unfortunately, offers no physical insights to the structure itself. Nevertheless, it can serve as a starting point to derive for a much more concise and physically meaningful equivalent circuit model. A variety of model-order reduction (MOR) techniques [2–5] have been proposed in the past to generate a low-order approximation of a given circuit. Most of these techniques were targeting to reduce the complexity of the circuit but not to provide physical insights. For examples, MOR techniques that can handle delays or preserve passivity have been proposed [6–9]. Circuit reduction approaches based on Gaussian elimination have also been developed [10–12].

Recently, a physics-based MOR technique called derived physically expressive circuit (DPEC) [13], which is based on the principle of Y-to- Δ transformation, has been developed. It uses the transformation to “absorb” all insignificant internal nodes so that the order-reduced circuit contains only the essences of the original. A major challenge to this technique is that it requires an inversion of the inductance matrix. This leads to the appearing of negative inductances to represent mutual couplings among inductors, and causes the order-reduced circuit physically meaningless. This drawback indeed limits the usefulness of the DPEC technique. Consequently, an alternative approach that does not require any matrix inversion nor generate any negative inductance is proposed in this work. This approach uses a more general Y-to- Δ transformation that can keep all mutual couplings intact during the reduction process. Hence, the inductance and potential matrices are not needed to be inverted in advance. By following a set of node removal criteria, a given partial element equivalent circuit can be reduced to one with fewer nodes but without sacrificing too much accuracy. This new physics-based MOR approach

Received 9 December 2015, Accepted 8 February 2016, Scheduled 3 March 2016

* Corresponding author: Lap Kun Yeung (lkyeung@msn.com).

The author is with the Department of Electronic Engineering, The Chinese University of Hong Kong, Shatin NT, Hong Kong, China.

works for problems that can be well modeled by a quasi-static PEEC, e.g., electrically small structures in free-space or in a multilayer substrate. Since all mutual couplings are kept intact, the proposed approach can provide physical insights to the structure being modeled.

2. THEORY

2.1. Conventional Formulation of PEEC

The partial element equivalent circuit technique is based on the concept of converting the mixed potential integral equation (MPIE) to a network representation that is suitable for solving in the circuit domain. By using a specific meshing scheme, a multi-conductor structure can be converted to a network consisting of discrete resistances, inductances, as well as capacitances, which are called partial elements. These partial elements compose an electromagnetically accurate equivalent circuit model in which additional components or circuit models, e.g., transistor circuit models, can easily be added in. The partial elements are first calculated by using either numerical integration procedures or analytical closed-form formulas. Then, the overall equivalent circuit is solved by a conventional circuit solver for various parameters of interest, e.g., scattering parameters.

The frequency-domain PEEC formulation starts from the MPIE of

$$\mathbf{E}(\mathbf{r}) = -j\omega \int_{V'} \overline{\overline{G_A}}(\mathbf{r}, \mathbf{r}') \cdot \mathbf{J}(\mathbf{r}') dv' - \nabla \int_{V'} G_\varphi(\mathbf{r}, \mathbf{r}') \rho(\mathbf{r}') dv', \quad (1)$$

where $\overline{\overline{G_A}}$ and G_φ are the dyadic and scalar Green's functions for magnetic vector and electric scalar potentials, respectively. For ease of explanation, only structures with infinitely thin conducting strips are considered. In this case, the volume integrals in Eq. (1) should change to surface integrals, and \mathbf{J} and ρ become the surface current and charge densities, respectively. In addition, without loss of generality, only the x-component in Eq. (1) is considered. By separately discretizing the current and charge densities using rectangular pulse functions, and having \mathbf{r} resided on the conducting strips, the discretized form of Eq. (1) is given by

$$\frac{J_x(\mathbf{r})}{\sigma} = -j\omega \sum_m \left(\int_{S'_m} G_A^{xx}(\mathbf{r}, \mathbf{r}') ds'_m \right) J_x^m - \frac{d}{dx} \sum_n \left(\int_{S'_n} G_\varphi(\mathbf{r}, \mathbf{r}') ds'_n \right) \rho_n, \quad (2)$$

from which a system of M equations is obtained by performing the Galerkin's matching procedure on Eq. (2) as

$$\frac{l_l}{\sigma w_l} I_x^l + \sum_m \frac{j\omega}{w_l w_m} \left(\iint G_A^{xx} ds'_m ds_l \right) I_x^m + \sum_n \frac{d}{dx} \frac{1}{w_l a_n} \left(\iint G_\varphi ds'_n ds_l \right) Q_n = 0, \quad (3)$$

for subscript $l = 1 \dots M$ where M is the number of inductive meshes. Notice that those pulse functions used for discretizing the current density are chosen to be the testing functions in this matching operation. Moreover, the integration domains and the arguments inside the Green's functions have been dropped for clarity. Whereas symbols w_l and w_m are the widths of inductive meshes l and m respectively, a_n is the area of capacitive mesh n . It is worth to mention that Eq. (3) is in the form of Kirchhoff's voltage law (KVL). The terms on the LHS represents, respectively, the resistive, inductive, and capacitive voltage drops across the matched inductive mesh l . In a more circuit-oriented form, Eq. (3) can be represented as (subscript x is dropped from now on).

$$R_l I_l + \sum_m j\omega L_{l,m} I_m + \sum_n \left(pp_{l,n}^+ - pp_{l,n}^- \right) Q_n = 0, \quad (4)$$

where a finite-difference approximation has been used for the derivative operation appearing at the last term. $L_{l,m}$ is the partial (self- or mutual) inductance, and pp 's (with sub-scripts) are the coefficients of potential. For ease of analysis, conductor loss R_i is combined with the corresponding self-inductance $L_{l,l}$ (or simply L_l), and replacing charge Q_n by an equivalent current, Eq. (4) can be rewritten as

$$\sum_m j\omega L_{l,m} I_m + \sum_n \frac{1}{j\omega} \left(pp_{l,n}^+ I_n - pp_{l,n}^- I_n \right) = 0, \quad (5)$$

where the substitution of $Q_n = I_n/j\omega$ has been used. Notice that L_l is now complex in value and has a frequency-dependent imaginary part. The second term in Eq. (5) represents the total induced voltage difference between the two ends (l^+ and l^-) of inductor l due to current I_n for all n . In fact, the voltage induced at a particular end (or equivalently, a circuit node) of an inductor is given by

$$V_k = \frac{I_1}{j\omega C_{k,1}} + \dots + \frac{I_{k-1}}{j\omega C_{k,k-1}} + \frac{I_k}{j\omega C_k} + \frac{I_{k+1}}{j\omega C_{k,k+1}} + \dots, \quad (6)$$

where k is the node index. Eq. (6) can be interpreted as a shunted-to-ground capacitor C_k (or $C_{k,k}$) connecting to node k . Additionally, this capacitor is mutually coupled to all other grounded capacitors connecting at different nodes with mutual capacitances of $C_{k,1}, C_{k,2}, \dots$ and so on. These capacitances are all frequency independent for the quasi-static case. As an illustration, consider a simple case of a single piece of conductor in free-space and its corresponding two-inductive-mesh partial element equivalent circuit as shown in Fig. 1. It can be seen that the circuit consists of two mutually coupled inductors and three mutually coupled capacitors. Notice that there are no couplings between inductors and capacitors.

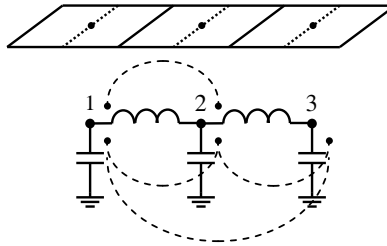


Figure 1. Partial element equivalent circuit of a short conducting strip.

In general, equivalent circuits generated by the PEEC analysis technique are described purely by mutually coupled inductors and mutually coupled capacitors only when the magnetic vector and electric scalar Green’s functions are well-defined. They are usually solved directly by using a circuit solver. This, however, leads to extremely time consuming matrix inversion operations since such circuits usually consist of a large number of elements. Therefore, it is desired to have their order reduced first. In fact, there are two advantages by carrying out the model-order reduction. Firstly, the matrices that require to be inverted are much smaller in size. Secondly, the simplified or reduced circuit is more concise and may provide insights to the structures that are being modeled.

2.2. Generalized Y-to-Δ Transformation

The reduction technique [10] based on the classical Y-to-Δ transformation suffers from one major issue. As the classical Y-to-Δ transformation cannot handle branches with couplings, the inductance matrix has to be first inverted to convert all mutual inductances to straight inductances. This leads to the generation of negative inductances. As an example, Fig. 2(a) depicts the conversion of a pair of coupled inductors to a network of six inductors with two of them being negative (dotted lines). This drawback indeed limits the usage of the technique to produce meaningful equivalent circuits. Here, an alternative approach that does not require any matrix inversion is proposed. Before the discussion of this new approach, it is better to clarify the terminology that will be used later in this paper. In this paper, a mutual coupling term is said to be inductive if it takes the form of $j\omega M_{ij,mn}$ where $M_{ij,mn}$ is called mutual inductance when the coupling is occurring between two inductors. On the other hand, a mutual coupling term is said to be capacitive if it takes the form of $1/j\omega C_{ij,mn}$ where $C_{ij,mn}$ is called mutual capacitance when the coupling is occurring between two capacitors. It is also worth to mention that conventional partial element equivalent circuits have only one (shunted-to-ground) capacitor at each node when using the formulation described in the previous section (see Fig. 1), or equivalently, when the Green’s functions in Eq. (1) are available.

Required mathematical expressions for the proposal MOR technique can be derived by considering the five-node sub-network shown on the LHS of Fig. 2(b). In this diagram, each branch consists of

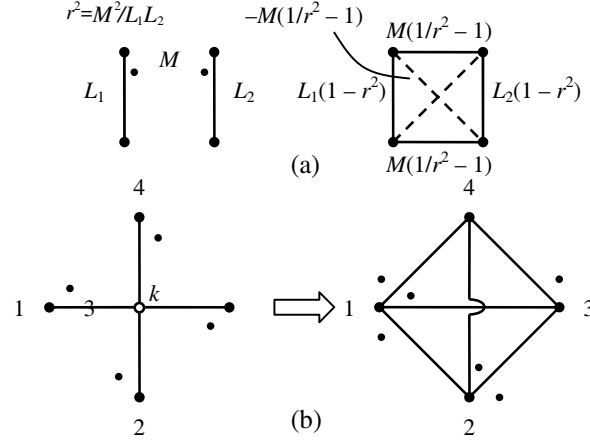


Figure 2. (a) Conversion of mutual inductance; and (b) internal node elimination process.

either a single inductor and/or a single capacitor, which may couple to other branches (including those “external” branches that are not shown in the figure). Specifically, for a conventional partial element equivalent circuit, one and only one of the branches, namely branch $2k$, should be a shunted-to-ground capacitor. The key operation here is to apply the Y-to- Δ transformation to eliminate node k and convert this sub-network to the four-node sub-network shown on the RHS of Fig. 2(b). Notice that the branches in this new sub-network may also couple to other internal or external branches. Mathematically, branch currents of the original five-node sub-network can be written as

$$I_{ik} = y_{ik}V_{ik} - \sum_{n \neq ik} \bar{z}_{ik,n}I_n - \dots, \quad (7)$$

for $i = 1 \dots 4$, where $\bar{z}_{ik,n} = z_{ik,n}/z_{ik}$ and “...” represents mutual coupling terms from all other (external) branches except (internal) branches $1k$ to $4k$. Making use of the fact that $I_{1k} + I_{2k} + I_{3k} + I_{4k} = 0$, V_k can be eliminated from the above system of equations and the branch currents can then be expressed as

$$I_{ik} = \sum_{j \neq i} \frac{y_{ik}y_{jk}}{y_t} V_{ij} + \bar{y}_{ik} \sum_j \sum_{n \neq jk} \bar{z}_{jk,n}I_n - \sum_{n \neq ik} \bar{z}_{ik,n}I_n + \dots, \quad (8)$$

for $i, j = 1 \dots 4$, where $\bar{y}_{ik} = y_{ik}/y_t$ and $y_t (= y_{1k} + y_{2k} + y_{3k} + y_{4k})$ is the total admittance of all branches that connect to node k . Now, consider the four-node sub-network, branch currents can be similarly written as

$$I_{ij} = y_{ij}V_{ij} - \Delta \bar{z}_{ij}I_{ij} - \sum_{n \neq ij} \bar{z}_{ij,n}I_n - \dots, \quad \text{with } i \neq j. \quad (9)$$

Notice that there is an extra term $\Delta \bar{z}_{ij}$ as compared to Eq. (7). Using the condition that

$$I_{ik} = \sum_{j \neq i} I_{ij}, \quad (10)$$

the branch currents of the original five-node sub-network can be expressed in terms of the new impedances from the four-node sub-network as

$$I_{ik} = \sum_{j \neq i} y_{ij}V_{ij} - \sum_{j \neq i} \Delta \bar{z}_{ij}I_{ij} - \sum_{j \neq i} \sum_{n \neq ij} \bar{z}_{ij,n}I_n - \dots, \quad (11)$$

The first two terms in Eq. (11) contain information about the branch (self-) impedances whereas the double summation term contains information about the internal and external mutual impedances.

Substituting Eq. (10) into Eq. (8) and then comparing with Eq. (11), the general expressions for these impedances can be summarized, respectively, as

$$z_{ij} = \frac{y_t}{y_{ik}y_{jk}} - 2z_{ik,jk} \tag{12a}$$

$$z_{ij,im} = z_{jk,mk} - z_{ik,jk} - z_{ik,mk} \tag{12b}$$

$$z_{ij,mn} = z_{ik,mk} + z_{jk,nk} - z_{ik,nk} - z_{jk,mk}$$

$$z_{ij,mn} = z_{ik,mn} - z_{jk,mn} \tag{12c}$$

for $i \neq j \neq m \neq n$ and $i, j, m, n = 1 \dots 4$ or $m, n \neq 1 \dots 4$ in (12c).

2.3. Model-Order Reduction

As discussed above, branches in a conventional partial element equivalent circuit consist of only two types, namely, a series inductor and a shunt capacitor. However, once a node is removed, a new branch type consisting of a shunt series-LC will be introduced. Therefore, in the following analysis, a shunt capacitor will be considered as a shunt series-LC with $L = 0$. According to Eq. (12a), if both branches ik and jk consist of a single inductor (see Fig. 3(a)), the resultant new branch ij should also be an inductor with inductance of

$$L_{ij} = \frac{L_{ik}L_{jk}}{L_t} (1 - \omega^2 L_t C_t) - 2M_{ik,jk}. \tag{13}$$

It is assumed that the condition of $|\omega^2 L_t C_t| \ll 1$ is valid at the maximum frequency of interest. On the other hand, if one branch (ik) is an inductor and the other branch (jk) is a series-LC (node j is the ground node) as depicted in Fig. 3(b), things become slightly more complicated. In this case, as the cross-branch coupling impedance is purely inductive (i.e., $z_{ik,jk} = j\omega X_{ik,jk}$), the new branch impedance should be

$$z_{ij} = \frac{1}{j\omega (L_t/L_{ik}) C_{jk}} + j\omega (\alpha L_{ik} - 2X_{ik,jk}), \tag{14}$$

where $\alpha = 1 + L_{jk}/L_t$. It can be seen that the new branch is also a series-LC with a capacitor of value $(L_t/L_{ik})C_{jk}$ in series with an inductor of value $\alpha L_{ik} - 2X_{ik,jk}$. As suggested by Eq. (13), the value of $|\omega^2 L_t C_t|$ can be used as an indicator to decide whether or not a given node should be removed. For

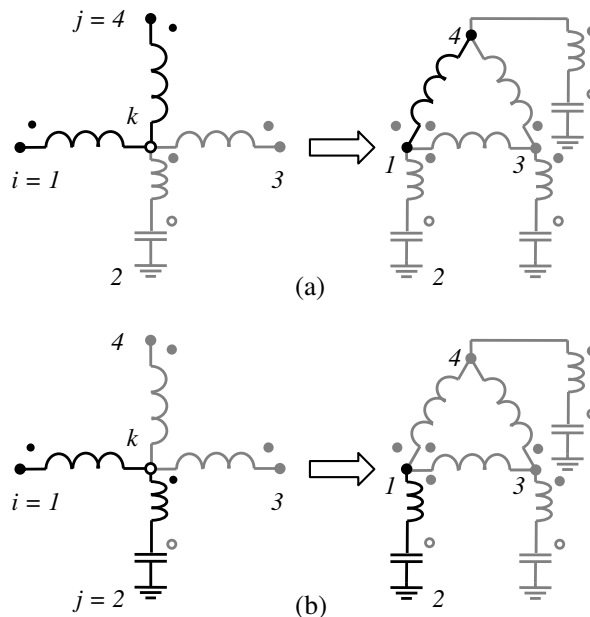


Figure 3. Generation of a new (a) inductance branch; and (b) series-LC branch.

example, given a node that has its value of $|\omega^2 L_t C_t|$ smaller than a pre-chosen small number δ at a specific cut-off frequency, this node can then be removed safely without introducing too much inaccuracy to the circuit model up to that frequency. In other words, the parameter δ is used for controlling the trade-off between accuracy and simplicity of the final order-reduced circuit. It is worth to mention that when removing a node, the majority of its influence to the circuit is transferred to other surrounding nodes. Finally, the case where both branches consisting of a series-LC is not considered here because there is only one such branch per node.

The internal coupling expressions shown in Eq. (12b) should be classified into three cases: i) inductor-branch coupling; ii) LC-branch coupling; and iii) cross-branch coupling. For the first case, both branches ij and im (or mn) consist of a single inductor, and therefore, the new mutual coupling is obviously inductive because all original involving branches ik , jk , and mk (or ik , jk , mk , and nk) are inductors (see Fig. 4(a)). The corresponding mutual inductance is equal to

$$\begin{aligned} M_{ij,im} &= M_{jk,mk} - M_{ik,jk} - M_{ik,mk} \\ M_{ij,mn} &= M_{ik,mk} + M_{jk,nk} - M_{ik,nk} - M_{jk,mk} \end{aligned} \quad (15)$$

For the second case in which both branches ij and im are a series-LC as in Fig. 4(b), the new mutual coupling calculation involves the original series-LC branch ik and inductor branches jk and mk . According to Eq. (12b), the new mutual impedance is given by

$$z_{ij,im} = j\omega M_{jk,mk} - j\omega X_{ik,jk} - j\omega X_{ik,mk}. \quad (16)$$

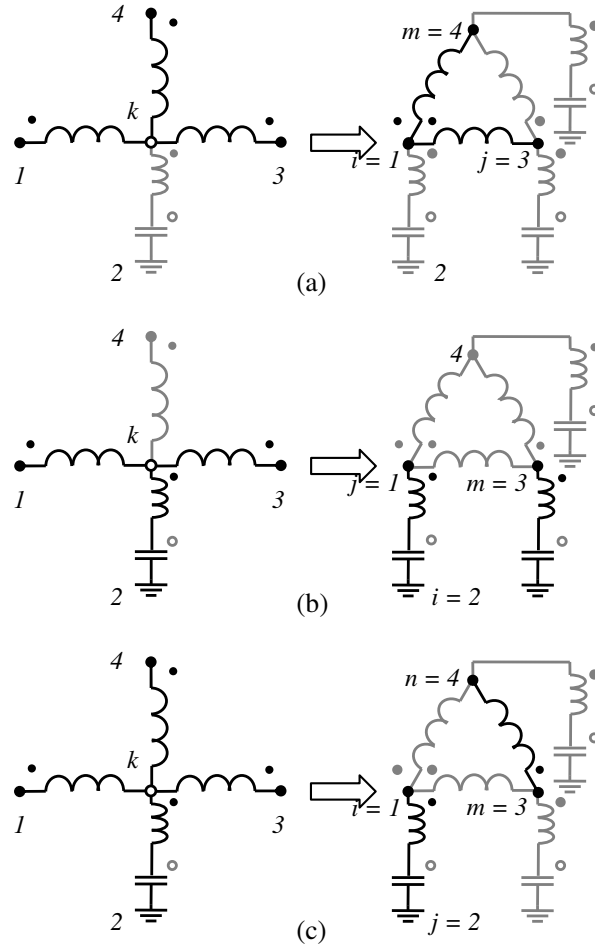


Figure 4. Generation of a new (a) internal inductor-branch coupling; (b) internal LC-branch coupling; and (c) internal cross-branch coupling.

Notice that the bottom expression of Eq. (12b) is not required in this case since there is always a common node (ground node) for all series-LC branches. It is seen that the coupling is purely inductive. Finally, for the third case where one branch (ij) is a series-LC and the other branch (im or mn) is an inductor (Fig. 4(c)), the mutual impedance is given by

$$\begin{aligned} z_{ij,im} &= j\omega X_{jk,mk} - j\omega X_{ik,jk} - j\omega M_{ik,mk} \\ z_{ij,mn} &= j\omega M_{ik,mk} + j\omega X_{jk,nk} - j\omega M_{ik,nk} - j\omega X_{jk,mk} \end{aligned} \quad (17)$$

which shows that the internal cross-branch coupling is also inductive. In summary, no matter in which case, all internal couplings are inductive.

The external coupling expression shown in Eq. (12c) should also be classified into three cases. For the inductor-branch coupling case, the new mutual inductance is simply equal to

$$M_{ij,mn} = M_{ik,mn} - M_{jk,mn}, \quad (18)$$

where branch mn is an external branch (see Fig. 5(a)). For the cross-branch coupling case, assuming branch ij is a series-LC and branch mn is an inductor (see Fig. 5(b)), the mutual impedance is given by

$$z_{ij,mn} = j\omega M_{ik,mn} - j\omega X_{jk,mn}, \quad (19)$$

which obviously is inductive. Finally, for the case of LC-branch coupling, things get a bit more complicated. The calculation involves an inductive coupling term and a capacitive coupling term. Again using Eq. (12c), the expression for this new mutual impedance is

$$z_{ij,mn} = j\omega X_{ik,mn} - j\omega M_{jk,mn} - \frac{1}{j\omega C_{jk,mn}}. \quad (20)$$

This mutual impedance contains a capacitive component as well as an inductive component as depicted in Fig. 5(c). Here, in addition to node j , either node m or node n is also grounded.

The newly converted four-node sub-network should be integrated back to the unmodified portion of the partial element equivalent circuit. This leads to the need for combining two branches of the same type in parallel. In general, the voltages across the two branches can be written as

$$\begin{pmatrix} V_{ij}^a \\ V_{ij}^b \end{pmatrix} = \begin{pmatrix} z_{ij}^a & z_c \\ z_c & z_{ij}^b \end{pmatrix} \begin{pmatrix} I_{ij}^a \\ I_{ij}^b \end{pmatrix} + \begin{pmatrix} \dots + z_{ij,n}^a I_n + \dots \\ \dots + z_{ij,n}^b I_n + \dots \end{pmatrix}. \quad (21)$$

Using the fact that both branch voltages are the same, the combined branch impedance and mutual impedance then become

$$z_{ij} = \frac{1}{y_t} \quad \text{and} \quad z_{ij,n} = \frac{y_{ij}^a + y_c}{y_t} \cdot z_{ij,n}^a + \frac{y_{ij}^b + y_c}{y_t} \cdot z_{ij,n}^b, \quad (22)$$

where those admittance parameters y 's are obtained by inverting the 2×2 impedance matrix in (21) (the first term on the RHS). Now, there are two cases need to be considered: i) the two branches are inductors; and ii) the two branches are series-LCs. The former is relatively easy to deal with and the resulting impedances are always inductive. On the other hand, the latter is slightly more complicated and should be further discussed. As shown in (20), the coupling of a newly generated series-LC to an external series-LC contains both inductive and capacitive components. In order to combine the two branches, the condition of $|\omega^2 \overline{LC}| \ll 1$ at the maximum frequency of interest should be assumed with $\overline{L} = L_a - L_b - 2M$, $\overline{C} - 1 = 1/C_a + 1/C_b - 2/C_M$, where L_a , L_b , M and C_a , C_b , C_M are the self- and mutual inductances as well as the self- and mutual capacitances of the two branches respectively. Under this condition, the capacitance and inductance of the new combined branch are obtained from the first expression of (23) as

$$C_{ij} = \left(\frac{\overline{C}}{C_a C_b} - \frac{\overline{C}}{C_M C_M} \right)^{-1}, \quad (23a)$$

$$L_{ij} = \left[\frac{\overline{C}}{C_b} L_a + \frac{\overline{C}}{C_a} L_b - \frac{2\overline{C}}{C_M} M \right] (1 + \omega^2 \overline{LC}) - \omega^2 (L_a L_b - M^2) \overline{C} (1 + \omega^2 \overline{LC}) - \frac{\overline{C}}{C_{ij}} \overline{L}. \quad (23b)$$

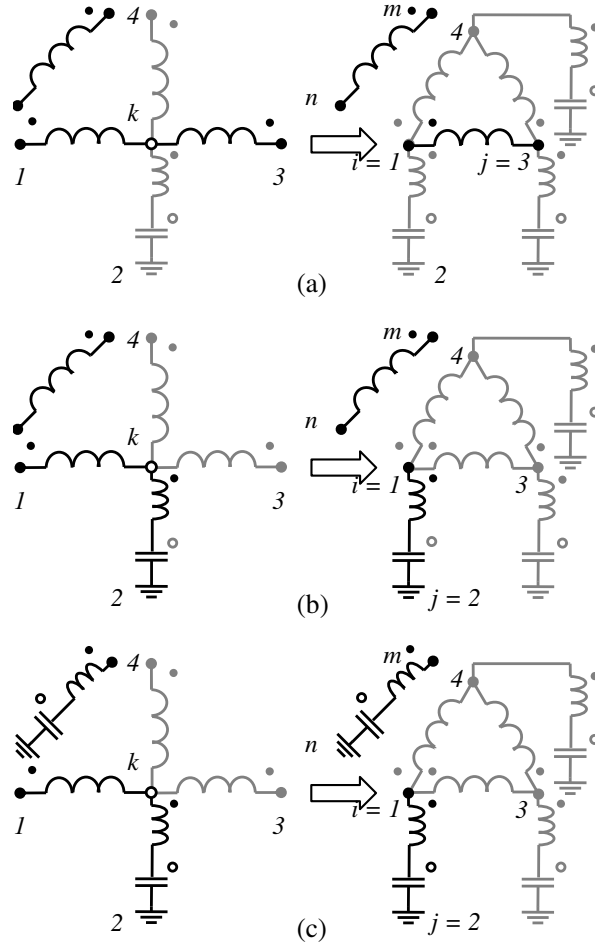


Figure 5. Generation of a new (a) external inductor-branch coupling; (b) external cross-branch coupling; and (c) external LC-branch coupling.

Notice that the condition of $|\omega^2(L_a L_b - M^2)\bar{C}|$ much less than the term inside the square bracket in Eq. (23b) is also required. The couplings of this new branch to other existing branches are given by the second expression of Eq. (22) in which the two weightings are

$$\frac{y_{ij}^a + y_c}{y_t} = \frac{\bar{C}}{\bar{C}_b} \cdot \frac{1 - \omega^2 \bar{L}_b \bar{C}_b}{1 - \omega^2 \bar{L} \bar{C}}, \quad (24a)$$

$$\frac{y_{ij}^b + y_c}{y_t} = \frac{\bar{C}}{\bar{C}_a} \cdot \frac{1 - \omega^2 \bar{L}_a \bar{C}_a}{1 - \omega^2 \bar{L} \bar{C}}, \quad (24b)$$

where parameters $\bar{L}_a = L_a - M$, $\bar{C}_a^{-1} = C_a^{-1} - C_M^{-1}$, $L_b = L_b - M$, and $\bar{C}_b^{-1} = C_b^{-1} - C_M^{-1}$.

While the impedances directly relating to the two combining branches are modified according to Eq. (22), the other impedances that are not directly related to these two branches should be modified according to the equation

$$z_{m,n} = z_{m,n} - \frac{y_{ij}^a y_{ij}^b - y_c^2}{y_t} \left(z_{ij,m}^a - z_{ij,m}^b \right) \left(z_{ij,n}^a - z_{ij,n}^b \right), \quad (25)$$

for all m and n except the two ij branches. Removing the inductors in series-LC branches is the final step of the reduction process. This can be done by using the following equations,

$$z_{ij'} = z_{ik} - z_{ik,j'k} - z_{j'k,ik} + z_{j'k} \quad (26a)$$

$$z_{ij',mj'} = z_{ik,mk} - z_{ik,j'k} - z_{j'k,mk} + z_{j'k}. \quad (26b)$$

$$z_{ij',n} = z_{ik,n} - z_{j'k,n} \tag{26c}$$

3. RESULTS

3.1. Embedded Bandpass Filters

Two multilayer bandpass filters [14, 15] embedded in a homogeneous substrate are used as examples to validate the proposed MOR algorithm. Both filters have a size of less than $4.32 \text{ mm} \times 2.04 \text{ mm} \times 0.55 \text{ mm}$. The first filter as shown in Fig. 6 consists of three layers of conductors above a large ground plane and buried inside a substrate of dielectric constant (ϵ_r) 7.8. The partial element equivalent circuit of this filter contains a total of 69 nodes. After the reduction with the control parameter δ and cut-off frequency set to 0.40 and 4 GHz respectively, a circuit of only 11 nodes is resulted. In terms of the number of state variables (node voltages and branch currents), it changes from 220 to 25. Fig. 6 also shows the scattering parameters obtained from these two circuits. It is seen that they are almost exactly the same as each other except the slight discrepancy from 3 GHz or above. Experimental measurements of the filter are also provided in the figure for comparison. The order-reduced circuit is depicts in Fig. 7. The node numbers in this circuit correspond to the numbered elements listed in Fig. 6. For simplicity, the coupling values between elements are not given. As a comparison, the time required for solving the original 69-node PEEC is $\sim 1.13 \text{ s}$ and that for the 11-node order-reduced circuit is $\sim 0.1 \text{ s}$. However, the model reduction process itself requires $\sim 1.92 \text{ s}$ to complete. Therefore, the proposed method allows the extraction of physical essences by trading off the computational efficiency. This is due to the fact that all mutual coupling terms among elements are required to be retained during the reduction process.

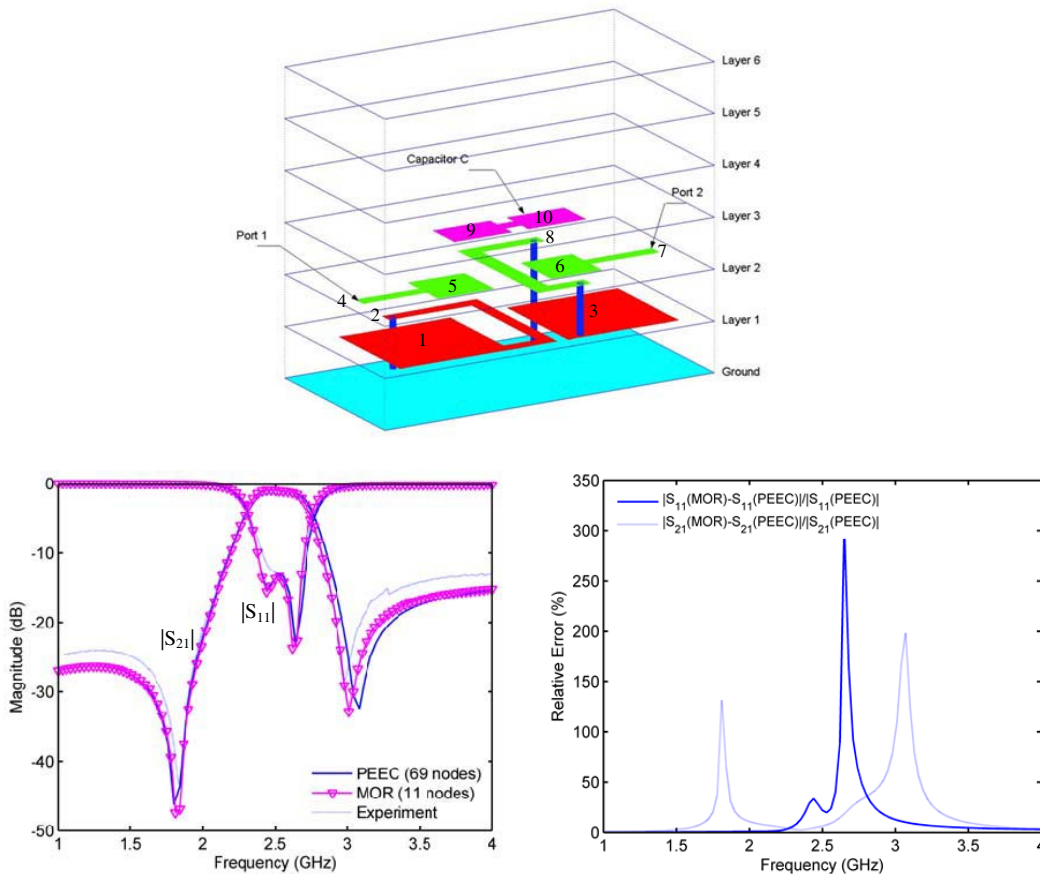


Figure 6. Embedded bandpass filter with two transmission zeros.

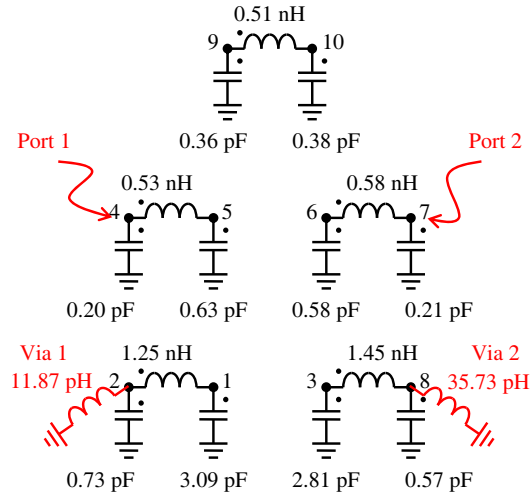


Figure 7. Order-reduced circuit for the two-zero bandpass filter.

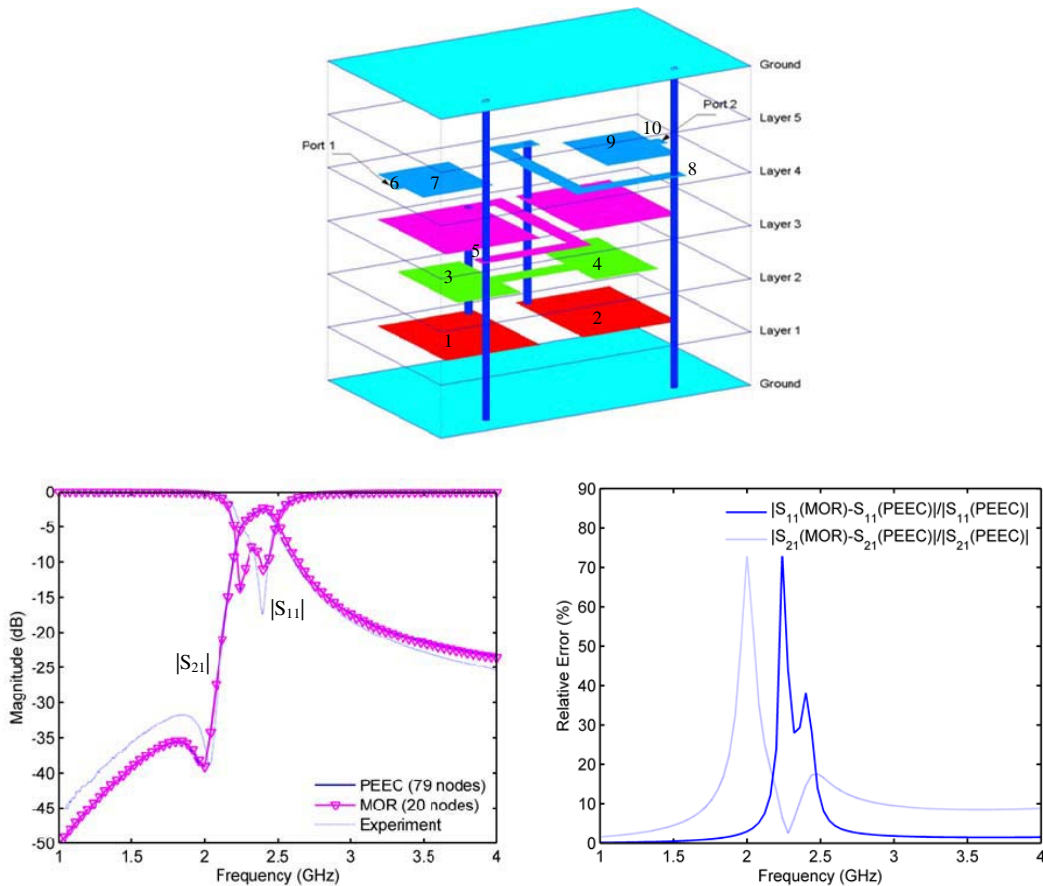


Figure 8. Bandpass filter enclosed between two ground planes.

The second example is a bandpass filter enclosed inside two large ground planes. It consists of four layers of conductors with buried vias connecting various different layers. The original PEEC contains 79 nodes whereas the order-reduced circuit contains only 20 nodes with the control parameter δ set to 0.15 and the cut-off frequency set to 4 GHz. The number of states variables changes from 253 to 68. Again

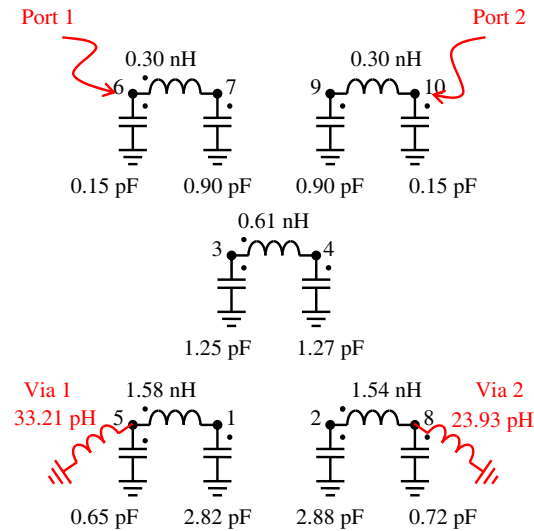


Figure 9. Order-reduced circuit for the second bandpass filter.

the two circuits give almost exactly the same scattering parameters (see Fig. 8). The circuit is further simplified to contain only 10 nodes (25 state variables) if the control parameter δ is to 0.4. The node numbers in this circuit (see Fig. 9) correspond to the numbered elements listed in Fig. 8. Experimental measurements are once again provided to valid the results from these two circuits. The original 79-node PEEC requires 1.66 s to solve, whereas the 20-node order-reduced circuit requires ~ 0.18 s but requires extra ~ 2.59 s for the reduction process.

From these two examples, it is seen that the proposed MOR algorithm indeed can eliminate redundant nodes and extract the essences of a given partial element equivalent circuit. Notice that there are some discrepancies between measurements and the simulation results. This is mainly because a homogeneous (half-space) substrate and an infinite ground plane are assumed in the simulations, but the prototype filters are embedded in a finite volume of substrate with a finite ground plane.

4. CONCLUSION

A new MOR algorithm which requires no matrix inversion is introduced in this work. By using the generalized Y-to- Δ transformation and making use of the features unique to the conventional PEEC, redundant internal nodes of a given partial element equivalent circuit can be absorbed without degrading the overall accuracy of the circuit model. Two frequency-domain examples are presented in the paper. Since all mutual couplings are kept intact, the final order-reduced circuit contains all essences of the original circuit.

ACKNOWLEDGMENT

This work was supported by University Grants Committee of Hong Kong under Grant AoE/P-04/08 and Grant GRF/418813.

APPENDIX A.

In general, the proposed MOR technique can be summarized as follows:

1. Search for the node with minimum value of $L_t C_t$ and $\omega^2 L_t C_t < 1$ at the maximum frequency of interest.
2. Perform the generalized y-to- Δ transformation on this node, and obtain the corresponding new branch elements using Eqs. (13) and (14).

3. Update the internal and external mutual couplings using Eqs. (15) to (20).
4. Combine all parallel branches and update the corresponding couplings using (23).
5. Update all other couplings by Eq. (25).
6. Remove cross-branch couplings using Eq. (26).
7. Repeat from step 1 until the node with minimum value of $L_t C_t$ does not satisfy the condition of $\omega^2 L_t C_t < 1$ at the maximum frequency of interest.

REFERENCES

1. Ruehli, A. E., "Equivalent circuit models for three dimensional multiconductor systems," *IEEE Trans. Microwave Theory Tech.*, Vol. 22, No. 3, 216–221, March 1974.
2. Pillage, L. T. and R. A. Rohrer, "Asymptotic waveform evaluation for timing analysis," *IEEE Trans. Computer-aided Design Integr. Circuits Syst.*, Vol. 9, No. 4, 352–366, April 1990.
3. Feldmann, P. and R. W. Freund, "Efficient linear circuit analysis by Pade approximation via the Lanczos process," *IEEE Trans. Computer-aided Design Integr. Circuits Syst.*, Vol. 14, No. 5, 639–649, May 1995.
4. Silveria, M., M. Kamon, I. Elfadel, and J. White, "A coordinate transformed Arnoldi algorithm for generating guaranteed stable reduced-order models of arbitrary RLC circuits," *Proc. ACM/IEEE Int. Conf. Computer-aided Design*, 288–294, San Jose, CA, 1996.
5. Odabasioglu, A., M. Celik, and L. T. Pileggi, "PRIMA: Passive reduced-order interconnect macromodeling algorithm," *IEEE Trans. Computer-aided Design Integr. Circuits Syst.*, Vol. 17, No. 8, 645–654, August 1998.
6. Ferranti, F., M. Nakhla, G. Antonini, T. Dhaene, L. Knockaert, and A. Ruehli, "Multipoint full-wave model order reduction for delayed PEEC models with large delays," *IEEE Trans. Electromagnetic Compat.*, Vol. 53, No. 4, 959–967, November 2011.
7. Ferranti, F., G. Antonini, T. Dhaene, and L. Knockaert, "Guaranteed passive parameterized model order reduction of the partial element equivalent circuit (PEEC) method," *IEEE Trans. Electromagnetic Compat.*, Vol. 52, No. 4, 974–984, November 2010.
8. Ferranti, F., G. Antonini, T. Dhaene, L. Knockaert, and A. E. Ruehli, "Physics-based passivity-preserving parameterized model order reduction for PEEC circuit analysis," *IEEE Trans. Components, Packaging Manufacturing Tech.*, Vol. 1, No. 3, 399–409, March 2011.
9. Ferranti, F., M. Nakhla, G. Antonini, T. Dhaene, L. Knockaert, and A. E. Ruehli, "Interpolation-based parameterized model order reduction of delayed systems," *IEEE Trans. Microwave Theory Tech.*, Vol. 60, No. 3, 431–440, March 2012.
10. Elias, P. J. H. and N. P. van der Meijs, "Extracting circuit models for large RC interconnections that are accurate up to a predefined signal frequency," *Proc. Design Automation Conf.*, 764–769, 1996.
11. Van Genderen, A. J. and N. P. van der Meijs, "Extracting simple but accurate RC models for VLSI interconnect," *Proc. Int. Symp. Circuits Syst.*, 2351–2354, 1988.
12. Sheeham, B. N., "TICER: Realizable reduction of extracted RC circuits," *Proc. Int. Conf. Computer-Aided Design*, 200–203, 1999.
13. Wang, J. and K. -L. Wu, "A derived physically expressive circuit model for multilayer RF embedded passives," *IEEE Trans. Microwave Theory Tech.*, Vol. 54, No. 5, 1961–1968, May 2006.
14. Yeung, L. K. and K. L. Wu, "A compact second-order LTCC bandpass filter with two finite transmission zeros," *IEEE Trans. Microwave Theory Tech.*, Vol. 51, No. 2, 337–341, February 2003.
15. Sutono, A., J. Laskar, and W. R. Smith, "Development of three dimensional integrated Bluetooth image reject filter," *IEEE MTT-S Int. Microwave Symp. Dig.*, 339–342, Boston, MA, 2000.